A C—C Bonded Phenoxyl Radical Dimer with a Zero Bond Dissociation Free Energy

Jessica M. Wittman, Rebecca Hayoun, Werner Kaminsky, Michael K. Coggins, James M. Mayer*

Department of Chemistry, University of Washington, Box 351700, Seattle, Washington 98195-1700, United States.

Supporting Information

Experimental:

General Considerations. Potassium ferricyanide, diethyl ether, and anhydrous carbon tetrachloride were purchased from Aldrich and used as received. Benzene, sodium hydroxide, and potassium bromide were purchased from EMD Millipore, Macron Chemical, and Fisher, respectively, and used as received. High purity acetonitrile was purchased from Burdick & Jackson and used as received. 2,6-di-*tert*-butyl-4-methoxyphenol was purchased from Aldrich and recrystallized from ethanol before use. All manipulations were performed using Schlenk line and glove box techniques with a nitrogen atmosphere unless otherwise specified. Elemental analysis was performed by Complete Analysis Laboratories, Inc.

Preparation of Dimer. The synthesis of 2,6-di-*tert*-butyl-4-methoxyphenoxyl radical (**^{t}Bu$_2$OMeArO$^•$**) was performed following literature procedures.[1] 10.8 g (0.0328 mol) of potassium ferricyanide was added to a frozen, degassed biphasic mixture of ^{t}Bu$_2$OMeArOH in benzene (0.11 M, 120 mL) and sodium hydroxide in water (1 M, 45 mL) under a N$_2$ atmosphere. The solution was left to stir for 2 hours at room temperature. The water layer was then removed with a syringe and the benzene layer was removed *in vacuo*. The product was extracted into diethyl ether and isolated by filtration and removal of solvent *in vacuo*, resulting in a purple oil. The spectra of this material matched the previously reported values. **^{t}Bu$_2$OMeArO$^•$** was dissolved in dry acetonitrile to give a deep purple solution, from which pale yellow crystals formed in the dark at -30 °C over days. The identity of the crystals as the dimer (**^{t}Bu$_2$OMeArO$^•$**)$_2$ was confirmed by X-ray crystallography and elemental analysis. Anal. (Calc.) C: 76.47 (76.55) H: 9.91 (9.85).

Determination of K_{eq} by UV-vis Measurements. A 0.10 M stock solution of **^{t}Bu$_2$OMeArO$^•$** in carbon tetrachloride (CCl$_4$) was prepared in the glove box. The stock solution

was diluted to give concentrations between 2 mM and 0.1 M and transferred to Kontes or septum-capped cuvettes. A 1-mm pathlength Kontes cuvette was used for concentrations above 0.08 M and a 2-mm pathlength Kontes cuvette was used for concentrations from 0.04-0.06 M. Variable temperature UV-vis spectra were obtained using a Hewlett-Packard 8453 diode array spectrophotometer with a Unisoku sample holder with a temperature controller. The absorbance at 605 nm was monitored in order to access higher ^{t}**Bu$_2$OMeArO$^\bullet$** concentrations. Figure S1 shows a Beer's Law plot of the absorbance at 605 nm for dilute solutions of ^{t}**Bu$_2$OMeArO$^\bullet$** in CCl$_4$ at room temperature. An extinction coefficient of $\varepsilon_{605\,nm} = 44 \pm 5$ M^{-1} s^{-1} was determined. Figure S2 shows the deviation from Beer's Law for solutions of ^{t}**Bu$_2$OMeArO$^\bullet$** at higher concentrations and lower temperatures. The absorbance values have been corrected for the different baselines of the different pathlength UV-vis cuvettes. The equilibrium constant for the dissociation of the dimer was determined by plotting the monomer concentration measured by UV-vis spectroscopy versus the [total]/[monomer] where [total] is the concentration of monomer if it was 100% dissociated (Equation S1, Figure S3). This relationship assumes a mass balance and that no precipitate is formed. Table S1 shows the slope and y-intercept values of the linear fit and the K_{eq} values for each temperature.

Equation S1.

$$K_{eq} = \frac{[\text{monomer}]^2}{[\text{dimer}]}$$

$$[\text{total}] = [\text{monomer}] + 2[\text{dimer}]$$

$$\frac{[\text{total}]}{[\text{monomer}]} = \frac{2}{K_{eq}}[\text{monomer}] + 1$$
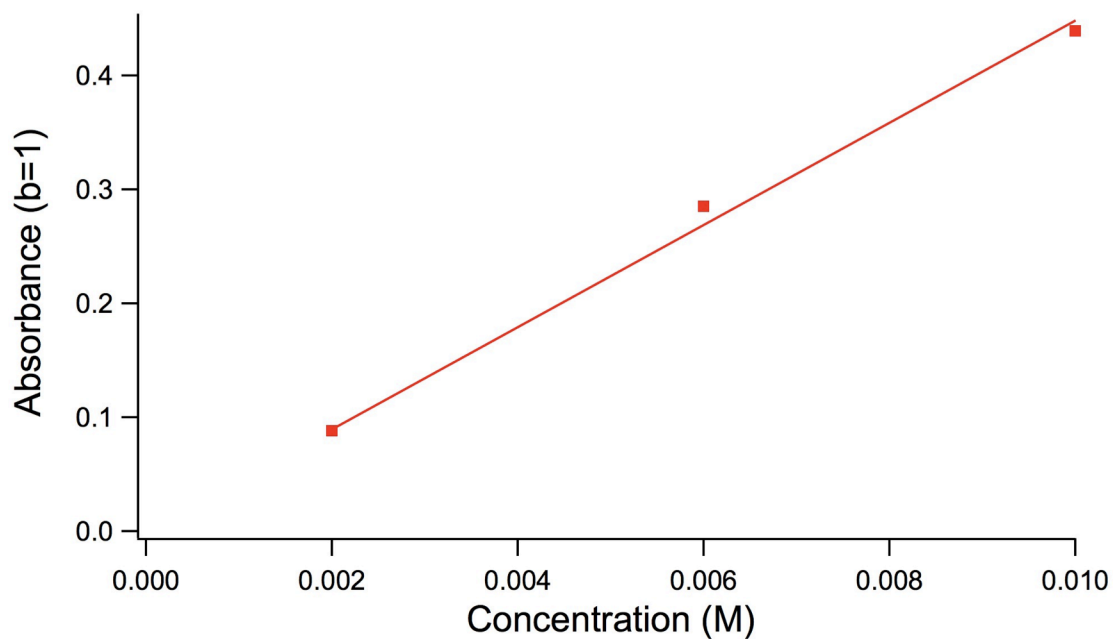
Figure S1. Beer's Law plot of $^tBu_2OMeArO^\bullet$ absorbance at 605 nm. The cell pathlength, b, was 1 cm for these solutions.
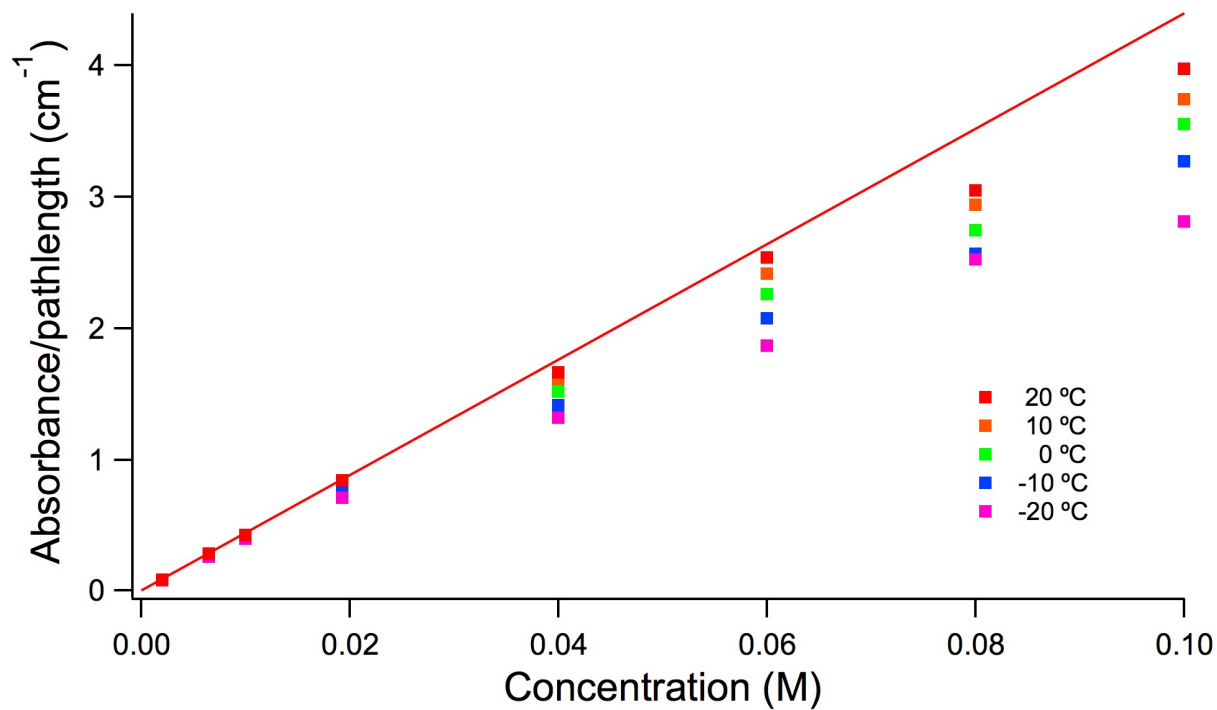
Figure S2. Deviation from Beer's Law of solutions of $^tBu_2OMeArO^\bullet$ at various temperatures. The slope of the red line is the ε_{605nm} determined from Figure S1.
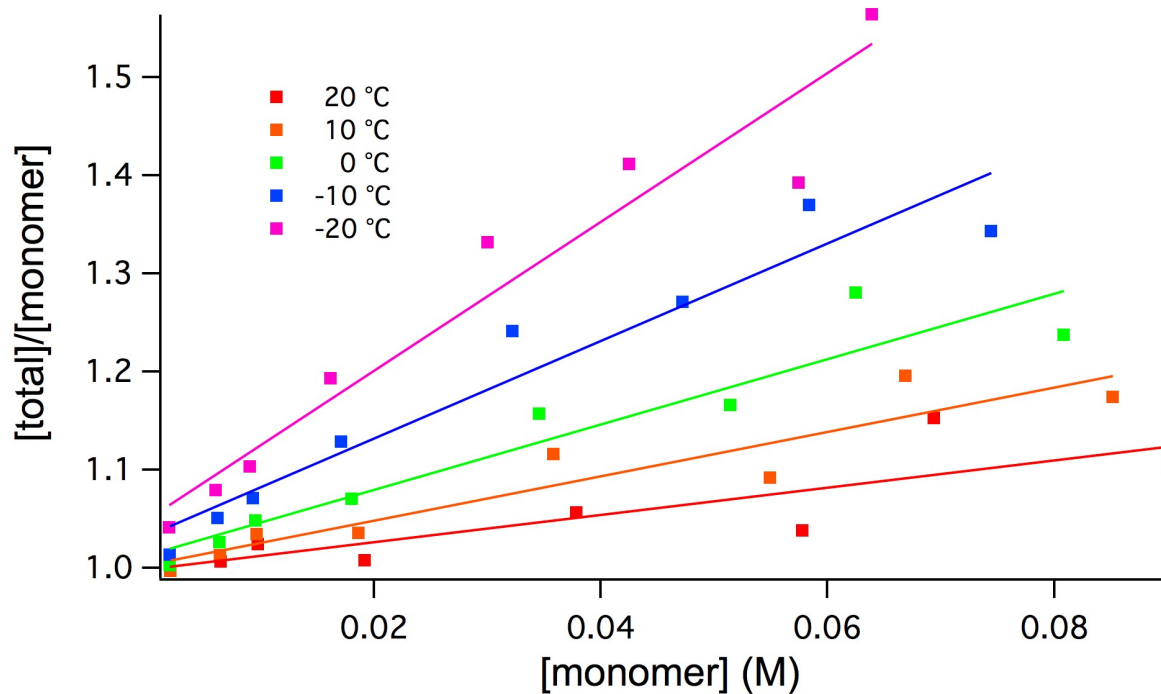
Figure S3. Plot of [monomer] vs. [total]/[monomer] for K_{eq} determination at temperatures 20 °C, 10 °C, 0 °C, -10 °C, and -20 °C.

Table S1. Slope and y-intercepts of the linear fits to the [total]/[monomer] vs. [monomer] plots and K_{eq} values for dimer dissociation each temperature.

Temperature (°C)	Slope (M^{-1})	y-intercept	K_{eq} (M^{-1})
20	1.4 ± 0.4	1.00 ± 0.02	1.44 ± 0.3
10	2.3 ± 0.3	1.00 ± 0.02	0.89 ± 0.2
0	3.3 ± 0.5	1.01 ± 0.02	0.60 ± 0.09
−10	5.0 ± 0.6	1.03 ± 0.02	0.40 ± 0.05
−20	7.6 ± 0.8	1.05 ± 0.03	0.26 ± 0.03

IR Methods for Characterization and Determination of K_{eq}. IR spectra were obtained using a Bruker Tensor 27 spectrophotometer. Background scans were collected after purging the sample chamber with nitrogen for 5 minutes. Sample scans were taken at 2 second intervals while purging with nitrogen. For each sample, the sample scan in which the carbon dioxide stretch near 3600 cm^{-1} was substracted out by the background was used.

Solid-state IR. A potassium bromide pellet of the dimer was prepared in the glove box and quickly removed to obtain an IR spectrum (Figure S5).

Solution IR. Solutions of **^{t}Bu$_2$OMeArO$^{\bullet}$** in CCl$_4$ were prepared and transferred to a PTFE-capped solution IR cell (Figure S6). A Beer's Law plot was generated for the absorbance of **^{t}Bu$_2$OMeArO$^{\bullet}$** at 1292 cm^{-1} at low concentrations (40 – 90 mM) for which the dimer IR signals are small (Figure S7). The extinction coefficient at 1292 cm^{-1} was used to calculate the [**^{t}Bu$_2$OMeArO$^{\bullet}$**] because the dimer has a relatively small extinction coefficient at this wavelength. Beer's Law plots for the absorbance of the dimer at 1646 cm^{-1} and 1667 cm^{-1} were also generated (Figure S8). The dimer concentrations used in the Beer's Law plots were calculated using the experimentally determined [**^{t}Bu$_2$OMeArO$^{\bullet}$**] and assuming a mass balance. The extinction coefficients at 1646 cm^{-1} and 1667 cm^{-1} were used to calculate the actual [dimer]. The equilibrium constant for dimer dissociation (K_{eq}) was determined by plotting [**^{t}Bu$_2$OMeArO$^{\bullet}$**]^2 vs. [dimer] (Figure S9). The K_{eq} was determined to be 1.29 ± 0.03 M.
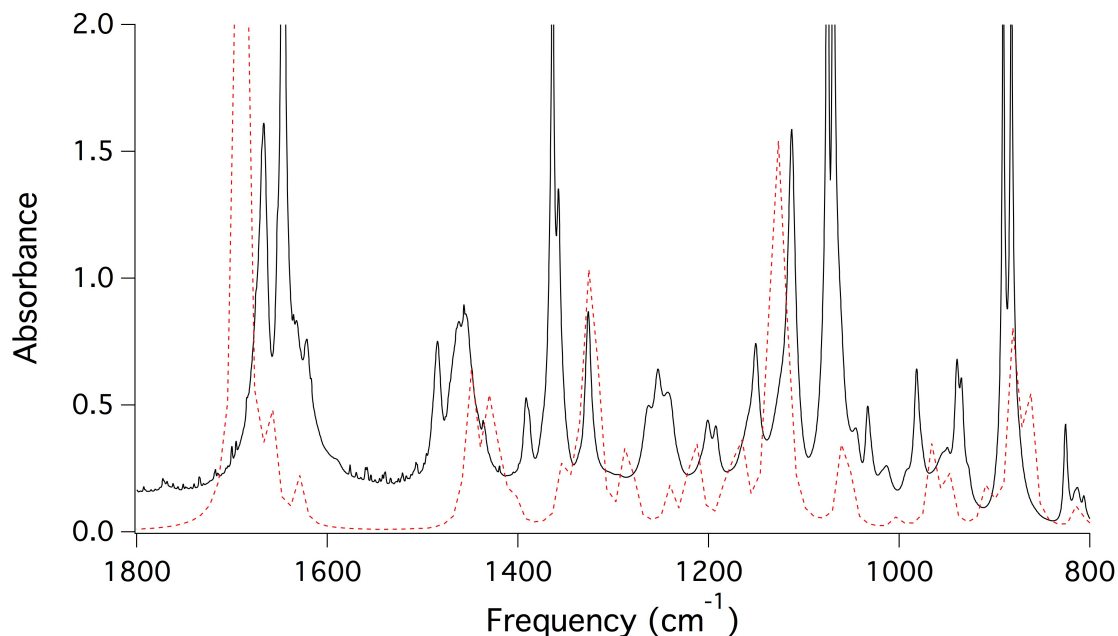
Figure S4. Solid state IR spectrum of dimer (black solid line) and IR frequencies calculated using M06-2X/6-31+G(2d,2p) (red dashed line). A scaling factor of 0.947 for the M06-2X functional from the NIST database was applied to the calculated IR frequencies.
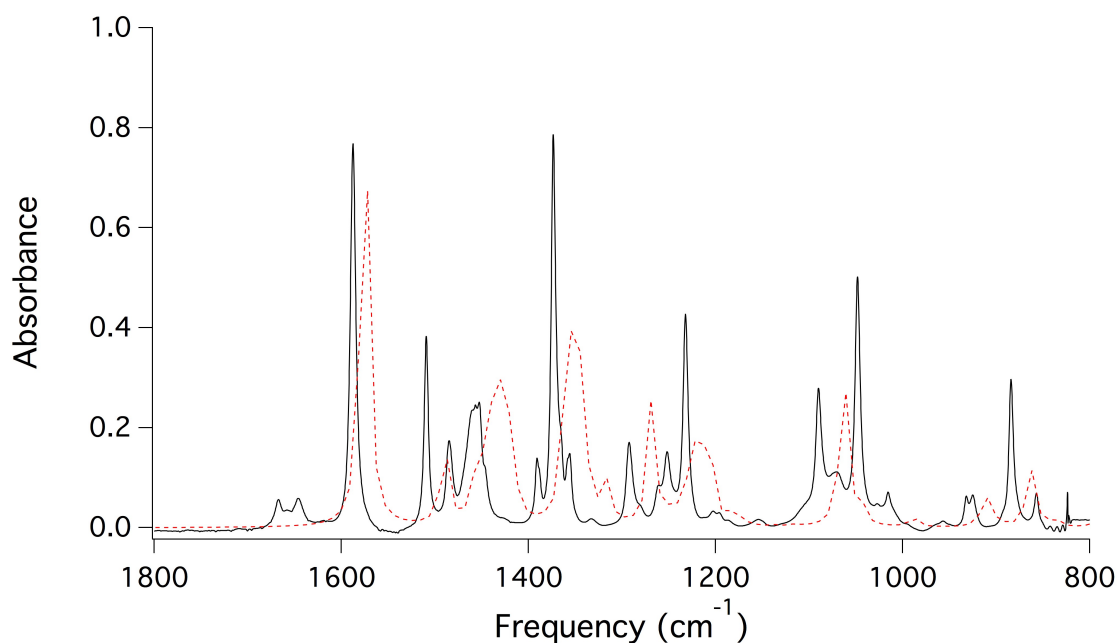
Figure S5. Solution IR spectrum of $^t\textbf{Bu}_2\textbf{OMeArO}^\bullet$ in CCl_4 (black solid line) and IR frequencies calculated using M06-2X/6-31+G(2d,2p) (red dashed line). A scaling factor of 0.947 for the M06-2X functional from the NIST database was applied to the calculated IR frequencies.

Table S2. Selected IR frequencies and assignments calculated using M06-2X with different basis sets and selected experimental IR frequencies.

Basis Set	Calculated Frequencies (cm^{-1})				
M06-2X/ 6-31G*	1640	1671.2	1671.4	1711	1031
M06-2X/ 6-31+G**	1633	1663.51	1663.53	1698	1033
M06-2X/ 6-31+G(2d,2p)	1629	1659.68	1659.75	1690	1032
Assignment[a]	C2=C3/C5=C6 asymmetric stretch	Mixed C2=C3/C5=C6/C1=O1 stretch	Mixed C2=C3/C5=C6/C1=O1 stretch	C1=O1 asymmetric stretch	C4-C4a symmetric stretch
Experiment[b]	1622, 1632, 1646, 1667				-

[a]From M06-2X calculations. [b]Experimental C=C/C=O IR frequencies have not been explicitly assigned. The C4-C4a stretching frequency may be IR inactive.
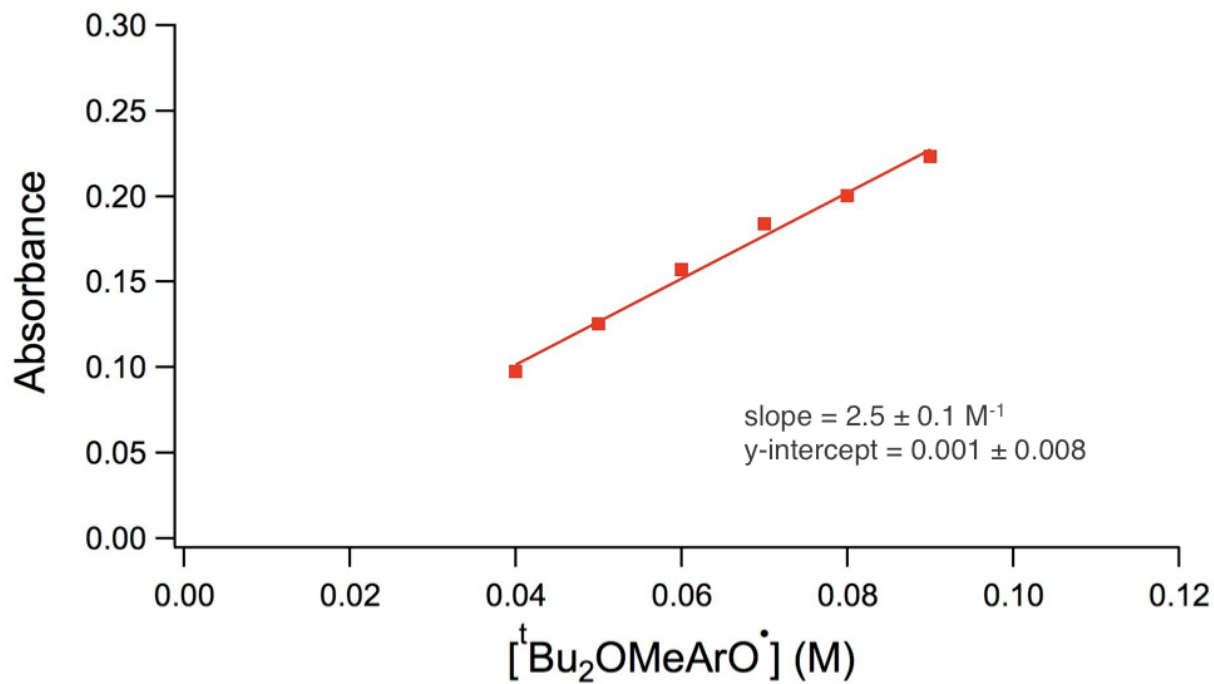
Figure S6. Beer's Law plot of **^{t}Bu$_2$OMeArO$^{\bullet}$** absorbance at 1292 cm^{-1}.

Figure S7. Beer's Law plot of dimer absorbance at 1646 cm^{-1} and 1667 cm^{-1}.

Figure S8. Plot of [^{t}**Bu$_2$OMeArO**$^\bullet$]^2 vs. [dimer].

DFT Calculations. All calculations were performed using Gaussian 09, Revision A.02.[3] Calculations were performed using the M06-2X functional and 6-31G*, 6-31+G**, and 6-31+G(2d,2p) basis sets. All basis sets provided similar results, and using larger basis sets led to greater agreement with experiment in the C4-C4a bond length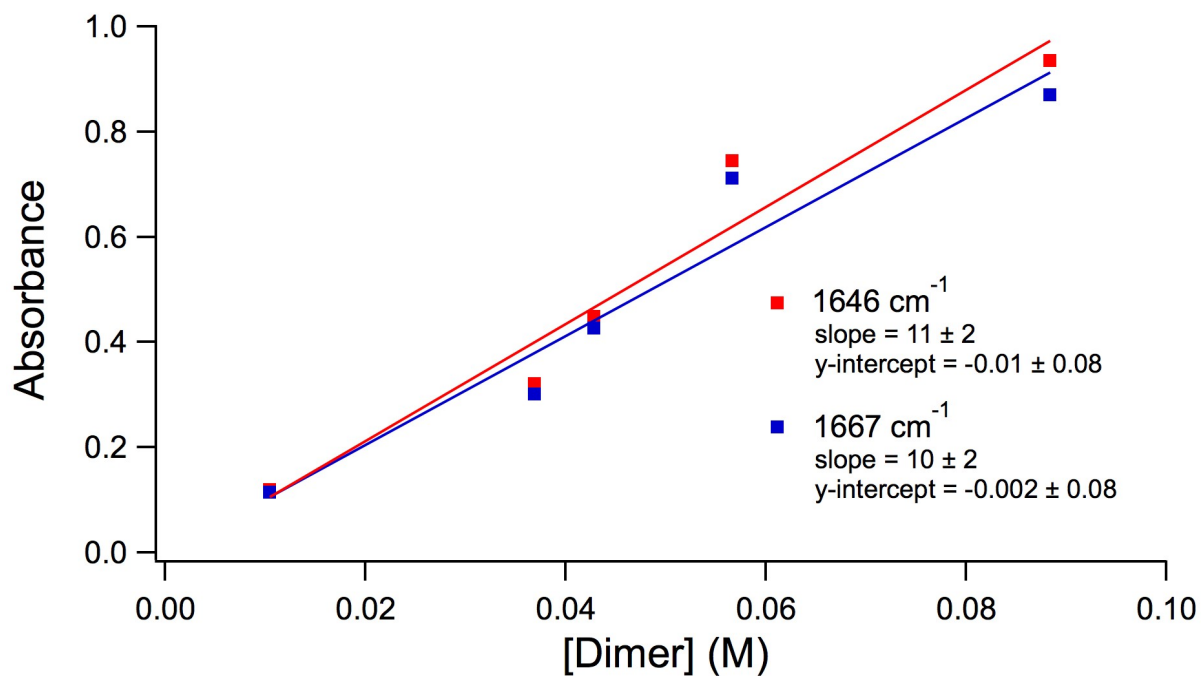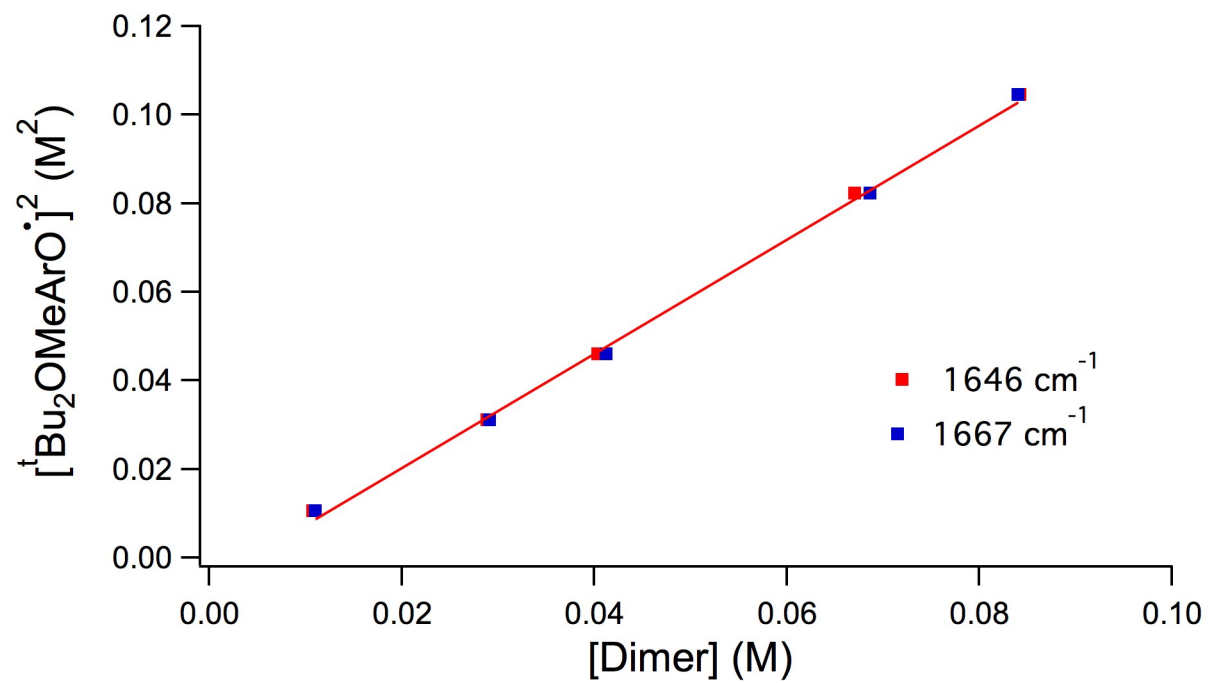, BDE, and IR frequencies. Calculations using the B3LYP functional provided C4-C4a bond lengths and BDEs which were in poor agreement with experiment. Geometry optimization calculations were performed for both the dimer and monomer. The optimized geometries for the dimer and monomer are tabulated (Tables S3 and S4, respectively) and absolute energies are reported in Table S5. Both geometries were checked by performing a wavefunction stability test (Stable=Opt), which indicated that both geometries were stable. Frequency calculations and thermochemical analyses were performed for the dimer and monomer. All geometries were confirmed to be local minima by IR frequency analysis (Table S5). The calculated force constant in internal coordinates of the C4-C4a bond of the dimer was determined from the frequency calculation and converted from Hartrees/($a_\circ^2$) to mDynes/Å (Table S5). The calculated sums of electronic and thermal enthalpies for the dimer and monomer were used to calculate the bond dissociation enthalpy (BDE) of the C4-C4a bond in the dimer (Table S5). The zero-point vibrational energies and calculated Gibbs free energy at 293 K (the temperature of the experiment) are also reported in Table S5. To estimate the stabilization energy of the dissociated dimer rearranging to the geometry of the monomer, a single point energy calculation was performed on the monomer with a geometry identical to half of the optimized dimer geometry. This is the expected geometry of the monomer after the dimer bond dissociation, but before relaxation to the monomer geometry. The absolute energy at this geometry is reported in Table S5. The calculated sums of electronic and thermal enthalpies were used to calculate the stabilization energy (Table S5).

Table S3. Optimized geometry of dimer in Cartesian coordinates (M06-2X/6-31+G(2d,2p)).

Center Label	Atomic Number	Coordinates (Å)		
		X	**Y**	**Z**
O1	8	4.25002	-0.00001	-0.87194
O2	8	-0.40544	0.00002	1.74447
C1	6	3.21538	-0.00001	-0.23487
C2	6	2.57273	-1.29105	0.18852
C3	6	1.3083	-1.24731	0.6149
H3	1	0.78088	-2.14233	0.92753
C4	6	0.48024	0	0.64387
C5	6	1.3083	1.24731	0.61488
H5	1	0.78089	2.14233	0.92749
C6	6	2.57274	1.29104	0.18851
C7	6	3.37588	2.58332	0.07654
C8	6	2.60526	3.76234	0.67943
H8A	1	1.67548	3.96098	0.13875
H8B	1	3.22108	4.6623	0.61662
H8C	1	2.36548	3.59284	1.73316
C9	6	3.64458	2.89968	-1.40623
H9A	1	2.70107	2.99124	-1.9519
H9B	1	4.24578	2.12374	-1.87613
H9C	1	4.1765	3.85249	-1.48288
C10	6	4.70618	2.44818	0.8373
H10A	1	5.25475	3.39231	0.78271
H10B	1	5.33172	1.66368	0.41451
H10C	1	4.52476	2.22468	1.89257
C11	6	3.37586	-2.58334	0.07653
C12	6	3.64454	-2.89968	-1.40625
H12A	1	2.70104	-2.99121	-1.95191
H12B	1	4.17645	-3.8525	-1.48292
H12C	1	4.24576	-2.12374	-1.87614
C13	6	4.70616	-2.44823	0.83728
H13A	1	5.3317	-1.66372	0.41451
H13B	1	5.25473	-3.39236	0.78266
H13C	1	4.52474	-2.22476	1.89257
C14	6	2.60522	-3.76237	0.6794
H14A	1	2.36543	-3.59287	1.73313
H14B	1	3.22105	-4.66232	0.61659
H14C	1	1.67545	-3.961	0.13871
C15	6	0.22967	-0.00004	3.00662

H15A	1	0.85303	-0.89062	3.14291
H15B	1	-0.56529	0.00018	3.75061
H15C	1	0.85341	0.8903	3.14281
O1a	8	-4.25004	0.00002	0.87195
O2a	8	0.40543	-0.00004	-1.74446
C1a	6	-3.21538	0.00001	0.23489
C2a	6	-2.57273	1.29105	-0.18851
C3a	6	-1.3083	1.2473	-0.6149
H3a	1	-0.78089	2.14232	-0.92753
C4a	6	-0.48025	-0.00001	-0.64386
C5a	6	-1.30832	-1.24732	-0.61487
H5a	1	-0.78091	-2.14234	-0.92748
C6a	6	-2.57276	-1.29104	-0.1885
C7a	6	-3.3759	-2.58333	-0.07653
C8a	6	-2.60525	-3.76234	-0.67943
H8Aa	1	-1.67547	-3.96096	-0.13875
H8Ba	1	-3.22107	-4.6623	-0.61662
H8Ca	1	-2.36548	-3.59282	-1.73316
C9a	6	-3.64459	-2.8997	1.40623
H9Aa	1	-2.70108	-2.99125	1.9519
H9Ba	1	-4.24581	-2.12378	1.87614
H9Ca	1	-4.1765	-3.85252	1.48287
C10a	6	-4.70619	-2.4482	-0.8373
H10Aa	1	-5.25475	-3.39234	-0.78273
H10Ba	1	-5.33175	-1.66372	-0.4145
H10Ca	1	-4.52476	-2.22468	-1.89257
C11a	6	-3.37585	2.58335	-0.07654
C12a	6	-3.6445	2.89975	1.40623
H12Aa	1	-2.70098	2.99125	1.95188
H12Ba	1	-4.17636	3.85259	1.48288
H12Ca	1	-4.24574	2.12385	1.87616
C13a	6	-4.70616	2.44825	-0.83728
H13Aa	1	-5.33173	1.66379	-0.41447
H13Ba	1	-5.2547	3.39241	-0.78269
H13Ca	1	-4.52476	2.22474	-1.89255
C14a	6	-2.60519	3.76234	-0.67946
H14Aa	1	-2.36543	3.59282	-1.73318
H14Ba	1	-3.22098	4.66232	-0.61665
H14Ca	1	-1.6754	3.96095	-0.13879
C15a	6	-0.22968	0.00002	-3.00661
H15Aa	1	-0.85305	0.8906	-3.14291
H15Ba	1	0.56528	-0.00019	-3.7506
H15Ca	1	-0.85342	-0.89032	-3.1428

Table S4. Optimized geometry of monomer in Cartesian coordinates (M06-2X/6-31+G(2d,2p)).

Center Label	Atomic Number	Coordinates (Å)		
		X	Y	Z
C1	6	-0.22514	-0.81255	-0.00001
C2	6	1.15377	-0.30234	0
C3	6	1.36616	1.05896	-0.00002
C4	6	0.28518	1.95296	-0.00003
C5	6	-1.04741	1.48916	-0.00002
C6	6	-1.33839	0.15373	0.00001
C7	6	2.31589	-1.29151	0.00001
H3	1	2.37222	1.44863	-0.00002
O2	8	0.4182	3.28885	-0.00005
H5	1	-1.81996	2.24629	-0.00002
C11	6	-2.77474	-0.35992	0.00003
O1	8	-0.44776	-2.03627	0.00004
C8	6	3.67221	-0.57706	-0.00002
C9	6	2.25084	-2.17376	1.26147
C10	6	2.25082	-2.17382	-1.2614
H9A	1	3.10709	-2.85415	1.27
H9B	1	2.3002	-1.55736	2.16348
H9C	1	1.33529	-2.76075	1.285
H8A	1	4.46691	-1.32648	0.00001
H8B	1	3.80627	0.04577	-0.88912
H8C	1	3.80628	0.04584	0.88904
H10A	1	3.10706	-2.85422	-1.26991
H10B	1	1.33526	-2.76081	-1.28488
H10C	1	2.30016	-1.55747	-2.16344
C12	6	-3.02637	-1.20775	1.26124
C13	6	-3.78494	0.79197	0.00001
C14	6	-3.02639	-1.20781	-1.26113
H12A	1	-4.06842	-1.54023	1.27063
H12B	1	-2.37953	-2.08242	1.28633
H12C	1	-2.854	-0.61356	2.16318
H13A	1	-4.79539	0.37698	0.00004
H13B	1	-3.68494	1.42178	0.88823
H13C	1	-3.68497	1.42173	-0.88825
H14A	1	-4.06844	-1.5403	-1.27049
H14B	1	-2.85404	-0.61366	-2.1631
H14C	1	-2.37955	-2.08247	-1.2862
C15	6	1.7213	3.84396	-0.00014

H15A	1	1.58427	4.9224	-0.00022
H15B	1	2.27396	3.54432	0.89412
H15C	1	2.27389	3.54417	-0.89441

Table S5. Comparison of calculated parameters using M-06/2X with various basis sets and experimental values.

	6-31G*	6-31+G**	6-31+G(2d,2p)	Experiment
Absolute Energy of Dimer (Hartrees)	-1471.08523502	-1471.16740116	-1471.23572129	-
Absolute Energy of Monomer (Hartrees)	-735.532518464	-735.574197421	-735.608646282	-
Absolute Energy of Single Point (Hartrees)	-735.475621360	-735.520594749	-735.554665529	-
C4-C4a Bond Length (Å)	1.6104	1.6079	1.6065	1.6055(23)
Zero-point Vibrational Energy of Dimer (kcal mol^{-1})	447.64914	444.10843	443.61766	-
Zero-point Vibrational Energy of Monomer (kcal mol^{-1})	222.95717	221.30382	220.98698	-
Zero-point Vibrational Energy of Single Point (kcal mol^{-1})	220.94276	219.94235	219.68701	-
Sum of electronic and thermal Enthalpies of Dimer (Hartrees)	-1470.332562	-1470.420008	-1470.489101	-
Sum of electronic and thermal Enthalpies of Monomer (Hartrees)	-735.157899	-735.202130	-735.237037	-
Sum of electronic and thermal Enthalpies of Single Point (Hartrees)	-735.103646	-735.150899	-735.185360	-
Bond Dissociation Enthalpy (kcal mol^{-1})	10.5	9.9	9.4	6.1
Stabilization Energy (kcal mol^{-1})	68.1	64.3	64.9	-
Bond Dissociation Free Energy at 293 K (kcal mol^{-1})	-2.0	-1.7	-2.3	-0.15
Total Entropy of Dimer (cal mol^{-1} K^{-1})	226.900	230.781	230.982	-
Total Entropy of Monomer (cal mol^{-1} K^{-1})	134.850	135.238	135.557	-
Force Constant (mDynes/Å)	3.607	3.57	3.59	-

Badger's Rule and Bond Length/Bond Strength Correlations. Badger's rule relates bond lengths to force constants according to equation 1,

$$r_e = (C_{ij}/k_e)^{\frac{1}{3}} + d_{ij} \tag{1}$$

where C_{ij} and d_{ij} are constant for a specific set of i-j bonded atoms.[3,4] The calculated force constant (k) of the C4-C4a bond in the phenoxyl radical dimer was compared to the force constants of typical C-C bonds in ethane, ethene, ethyne, and benzene (Table S2). The bond lengths were plotted versus $k^{-1/3}$ to determine whether the C4-C4a dimer bond follows the same linear relationship proposed by Badger (Equation 1) as the C-C bonds in ethane, ethene, ethyne, and benzene (Figure 4B in the manuscript).[3,4] The $k^{-1/3}$ values of the C4-C4a dimer bond is in good agreement with the trend predicted by the ethane, ethene, ethyne, and benzene C-C bonds

Table S6. Experimental bond lengths and bond dissociation energies (BDEs) and experimental and calculated force constants of C-C bonds in ethane, ethene, ethyne, benzene, and the dimer.

	Bond Length (Å)	BDE (kcal mol^{-1})	Force Constant (mDyne/Å)
H_3C-CH_3	1.5351[a]	89.68[a]	4.5[b]
$H_2C=CH_2$	1.339[a]	172.2[a]	9.7[b]
$HC\equiv CH$	1.203[a]	229.9[a]	15.6[b]
C_6H_6	1.39[c]		7.6[b]
Dimer C4-C4a bond	1.6055(23)[d]	6.1[e]	3.6[f]

[a]ref[5]. [b]ref[6]. [c]ref[7]. [d]Crystallographic value. [e]Determined from van't Hoff plot. [f]M06-2X/6-31+G(2d,2p).

Crystallographic Information. A colorless plate, measuring 0.35 x 0.20 x 0.02 mm^3 was mounted on a glass capillary with oil. Data was collected at -173 °C on a Bruker APEX II single crystal X-ray diffractometer, Mo-radiation.

The crystal-to-detector distance was 40 mm and exposure time was 10 seconds per degree for all sets. The scan width was 0.5°. Data collection was 99.9% complete to 25° in ϑ. A total of 46501 (merged) reflections were collected covering the indices, h = -13 to 13, k = -24 to 24, l = -19 to 19. 3524 reflections were symmetry independent and the R$_{int}$ = 0.0480 indicated that the data was good (average quality 0.07). Indexing and unit cell refinement indicated a C - centered monoclinic lattice. The space group was found to be C 2/c (No.15).

The data was integrated and scaled using SAINT, SADABS within the APEX2 software package by Bruker.[8]

Solution by direct methods (SHELXS, SIR97[9]) produced a complete heavy atom phasing model consistent with the proposed structure. The structure was completed by difference Fourier synthesis with SHELXL97.[10,11] Scattering factors are from Waasmair and Kirfel[12]. Hydrogen atoms were placed in geometrically idealised positions and constrained to ride on their parent atoms with C---H distances in the range 0.95-1.00 Angstrom. Isotropic thermal parameters U$_{eq}$ were fixed such that they were 1.2U$_{eq}$ of their parent atom Ueq for CH's and 1.5U$_{eq}$ of their parent atom U$_{eq}$ in case of methyl groups. All non-hydrogen atoms were refined anisotropically by full-matrix least-squares.

Table S2: Crystallographic data.

Empirical formula	C30 H46 O4
Formula weight	470.67
Temperature	100(2) K
Wavelength	0.71073 Å
Crystal system	Monoclinic
Space group	C 2/c
Unit cell dimensions	a = 10.2918(9) Å α= 90°.
	b = 18.727(2) Å β= 94.587(4)°.
	c = 14.6697(12) Å γ = 90°.
Volume	2818.3(5) Å^3
Z	4
Density (calculated)	1.109 Mg/m^3
Absorption coefficient	0.071 mm^{-1}
F(000)	1032
Crystal size	0.30 x 0.15 x 0.14 mm^3
Theta range for data collection	2.17 to 28.40°.
Index ranges	-13<=h<=13, -24<=k<=24, -19<=l<=19
Reflections collected	46501
Independent reflections	3524 [R(int) = 0.0480]
Completeness to theta = 25.00°	99.9 %
Max. and min. transmission	0.9901 and 0.9789
Refinement method	Full-matrix least-squares on F^2
Data / restraints / parameters	3524 / 0 / 161
Goodness-of-fit on F^2	1.078
Final R indices [I>2sigma(I)]	R1 = 0.0490, wR2 = 0.1359
R indices (all data)	R1 = 0.0575, wR2 = 0.1472
Largest diff. peak and hole	0.567 and -0.301 e.Å^{-3}

References:

(1) Manner, V. W.; Markle, T. F.; Freudenthal, J. H.; Roth, J. P.; Mayer, J. M. *Chem. Commun.* **2008**, 256-258.

(2) Gaussian 09, Revision A.1, M. J. Frisch, G. W. Trucks, H. B. Schlegel, G. E. Scuseria, M. A. Robb, J. R. Cheeseman, G. Scalmani, V. Barone, B. Mennucci, G. A. Petersson, H. Nakatsuji, M. Caricato, X. Li, H. P. Hratchian, A. F. Izmaylov, J. Bloino, G. Zheng, J. L. Sonnenberg, M. Hada, M. Ehara, K. Toyota, R. Fukuda, J. Hasegawa, M. Ishida, T. Nakajima, Y. Honda, O. Kitao, H. Nakai, T. Vreven, J. A. Montgomery, Jr., J. E. Peralta, F. Ogliaro, M. Bearpark, J. J. Heyd, E. Brothers, K. N. Kudin, V. N. Staroverov, R. Kobayashi, J. Normand, K. Raghavachari, A. Rendell, J. C. Burant, S. S. Iyengar, J. Tomasi, M. Cossi, N. Rega, J. M. Millam, M. Klene, J. E. Knox, J. B. Cross, V. Bakken, C. Adamo, J. Jaramillo, R. Gomperts, R. E. Stratmann, O. Yazyev, A. J. Austin, R. Cammi, C. Pomelli, J. W. Ochterski, R. L. Martin, K. Morokuma, V. G. Zakrzewski, G. A. Voth, P. Salvador, J. J. Dannenberg, S. Dapprich, A. D. Daniels, Ö. Farkas, J. B. Foresman, J. V. Ortiz, J. Cioslowski, and D. J. Fox, Gaussian, Inc., Wallingford CT, 2009.

(3) Badger, R. M. *J. Chem. Phys.* **1934**, *2*.

(4) Badger, R. M. *J. Chem. Phys.* **1935**, *3*, 710-714.

(5) Zavitsas, A. A. *J. Phys. Chem. A* **2003**, *107*, 897-898.

(6) Robinson, E. A. L., M. W. *Can. J. Chem.* **1963**, *41*, 2988-2995.

(7) Haynes, W. M. *CRC Handbook of Chemistry and Physics*; 93 ed.; CRC Press: Baco Raton, FL, 2012.

(8) Bruker (2007) APEX2 (Version 2.1-4), SAINT (version 7.34A), SADABS (version 2007/4), BrukerAXS Inc, Madison, Wisconsin, USA.

(9) (a) Altomare, A.; Burla, C.; Camalli M.; Cascarano L.; Giacovazzo C.; Guagliardi A.; Moliterni A.G.G.; Polidori G.; Spagna R. J. *Appl. Cryst.* **1999**, *32*, 115-119; (b) Altomare, A., Cascarano, G., Giacovazzo, C., Guagliardi, A., J. *Appl. Cryst.* **1993**, *26*, 343.

(10) Sheldrick, G. M. SHELXL-97: Program for the Refinement of Crystal Structures 1997 University of Gottingen, Germany.

(11) Mackay, S.; Edwards, C.; Henderson, A.; Gilmore, C.; Stewart, N.; Shankland, K.; Donald, A.; MaXus: a computer program for the solution and refinement of crystal structures from diffraction data. University of Glasgow, Scotland, 1997.

(12) Waasmaier, D.; Kirfel, A. *Acta Crystallographica Section A* **1995**, *51*, 416-431.